Development of an environmental high-voltage electron microscope for reaction science

Nobuo Tanaka, Jiro Usukura, Michiko Kusunoki, Yahachi Saito, Katuhiro Sasaki, Takayoshi Tanji, Shunsuke Muto , and Shigeo Arai.

Ecotopia Science Institute and Graduate School of Engineering, Nagoya University
Chikusa-ku, Nagoya, 464-8603, Japan

*To whom correspondence should be addressed. E-mail: a41263a@nucc.cc.nagoya-u.ac.jp.

Abstract

Environmental transmission electron microscopy is recently of a great interest as well as ultra-high resolution observation using aberration correctors. This method is a kind of extension of so-called "in-situ electron microscopy" performed since the 1970's. It nowadays focuses on dynamic observation with atomic resolution in gaseous atmosphere and liquids. Since 2007, Nagoya university has developed a new 1 MV high voltage (scanning) transmission electron microscope, where nano-materials can be observed in conditions of gases, liquids and illuminating lights and mechanical operation as well as in three-dimension by using electron tomography.

Keyword

Environmental high-voltage electron microscope; reaction science; in-situ observation; 3D observation; TEM/STEM.

Received : 10, October, 2012, **Accepted** :

1. Introduction

Recently energy and environmental problems are our important issues resolved smartly as "Green Technology" or "Green Manufacturing"[1]. We have to pay attention from the first step of development of materials and their devices, because the previous methods for estimation and treatments after the production cost so much and not fitted for our concerns. In order to assess the development, we need to observe and analyze model samples in actual usage/reaction conditions. For this purpose, the necessity of environmental and in-situ observation is increased for structural and elemental analyses

in atomic dimensions.

Transmission electron microscopy (TEM) is one of the best useful tool for estimation of nano-materials and nano-devices. There are, however, several limitations in the TEM such as (1) necessity of thin samples less than 0.1 micrometer, (2) observation in vacuum, and (3) projected images of samples in place of three-dimensional structural information. The problems have been studied for a long time since 1970's, and various kinds of techniques were developed in order to decrease the limitations. Since 2007, a new high voltage scanning transmission electron microscope(HV-STEM) equipped with an open-type environmental cell, largely tilting holders, high-sensitivity TV cameras and an imaging filter for electron energy loss spectroscopy(EELS) and energy-filtered imaging has been developed in Nagoya University, which was named "Reaction Science High-Voltage Electron Microscope (RSHVEM)"[2]. In this paper, we describe the details and some applications.

2. Details of the instrument

Figure 1 shows an illustration of a general view of the RSHVEM (JEM-1000K RS). The height of a tank housing the accelerating tube is 6.7 m, and the length of the microscope column is 3.6 m. The basement housing an anti-vibration stage is 3.7m depth. The electron gun uses a LaB_6 thermionic cathode, whose chamber is evacuated by two dedicated ion pumps of 20 l/s. in order to extend the life time. At 1 MV, we can observe samples of about 5 micrometer thickness for aluminum. The three-stage condenser lens system focuses an electron beam down to less than 1 nm, which gives bright field and dark field STEM images and elemental mapping images using EELS.

The most important specification of the present RSHVEM is the availability of high-resolution observation at 1 MV in various kinds of gaseous conditions of a few tenth of atmosphere, for example, 13,300 Pa(=100 Torr). The other specifications are 1 MV maximum accelerating voltage, less than 0.15 nm point-to point resolution of TEM, less than 1 nm STEM resolution and less than 1.5 eV energy resolution in EELS, and ± 70 degree tilting angles of ordinary sample holders and ±180 tilting degree by using a dedicated holder for electron tomography. Particular focus was made on the development of a new environmental cell for HVEM with keeping the point-to-point resolution of images.

There are basically two kinds of techniques for environmental observation in gaseous atmosphere. One is with use of the closed type cell, where amorphous carbon or silicon nitride membrane films are used for separation between the atmospheric gases around samples and vacuum in other part of the column[3]. Another is by using the open type

cell without the membrane and with differential pumping[4-8]. We adopted the latter for keeping the image resolution and avoiding contamination and damages of the membrane.

For realizing the environmental specifications, we have developed a new side-entry sample holder without a stopper at the opposite side of a goniometer, which enabled inserting the environmental cell in the same side. In this case, ordinary sample holders can be used. In extracting the cell, we can use the instrument as an ordinary HVEM in vacuum condition. The time for insertion/extraction is a few minutes. For adopting the open cell system, three-stage differential pumping system around the objective lens was newly developed, which composed of five turbo molecular pumps and a scrolled pump. Figure 2 shows vacuum characteristics from gas introduction to re-evacuation. After the gas environment, the time to vacuum less than 10^{-3} Pa, so-called rumpling time, is less than 10 min.

The image recording system consists of three CCD cameras for recording low magnification images and electron diffraction patterns(Hamamatsu; 2k x 2k pixels), high-resolution images(Gatan; ORIUS; 2k x 2k pixels) and EEL spectra and the energy-filtered images(Gatan; Imaging filter (GIF); 2k x 2k pixels).

3. Observation for confirming the basic specifications

Figure 3 shows a high-resolution TEM image of a [110] oriented cubic SiC crystal recorded at 1 MV, where the dumbbell structure composed of silicon(Si) atomic columns and carbon(C) ones are clearly discriminated. The separation of the dumbbell is 0.109 nm.

For EELS at 1 MV, recorded the zero-loss peak of 0.87 eV, which shows a good performance of the GIF spectrometer and a high stability of total electric systems of the present RSHVEM. Figure 4 shows an energy filtered image of a particle of Ce_2O_3. Using the M-edge of cerium (ΔE=833 eV), we have a sufficient image contrast, which shows a distribution of Ce atoms in the particle.

Figure 5 shows high-resolution lattice images of a [001] oriented gold(Au) film in vacuum condition(a) and gaseous one(b). Even at 11,000 Pa of nitrogen gas, we can clearly observed (200) lattice fringes of gold. This is the world-top datum of image resolution for environmental TEM in gaseous conditions by using the open-type environmental cell. The reason of the achievement is that (1)we use high-energy incident electrons which pass through gas layers without so much inelastic scattering, and (2) relatively thin gas layers realized by the new design of an environmental cell, which is different from previous one[4-8]

4. Examples of application of the RSHVEM

(A) Observation in gaseous conditions

(A-1) Cu particles on silica particles

The copper (Cu) particles were prepared by vacuum-deposition of Cu onto commercial silica(SiO_2) powders inside the RSHVEM. A specially developed sample holder having two filaments, one of which is for sample support and heating, other, for metal deposition, was used[9]. Figure 6 shows a low-magnification bright field image of the sample with Cu deposited. First, the in-situ oxidation was performed at 700 C by introducing oxygen gas of 1 Pa. Electron microscope images and EELS spectra were recorded simultaneously. In the micrographs and the corresponding diffraction patterns, copper mono-oxide was detected as well as copper. In the micrographs, a change of the image contrast from multiple twinned Cu particles to flat-contrast particles was observed. Figures 7(a) and (b) show series of EELS during the oxidation process. In the duration time, K-edges of oxygen was evolved. Comparing the standard spectra of Cu, Cu_2O and CuO, the final state of the particles obtained in the RSHVEM was determined to be CuO. Figure 7(c) shows the reduction process of the oxidized particles by introducing a 30 Pa gas composed of 5% of H_2 and 95% of N_2 at 700 C. The K-edges of oxygen is gradually decreased, and finally we obtained pure Cu particles. While the oxidation and reduction processes, the particle shape is almost similar. For tin(Sn) particles also, we have observed a transition from the particles in liquid state to solid particles of tin-oxide(SnO) at 250 C by introducing oxygen gas of 5×10^{-5} Pa[2].

(A-2) Catalytic reaction of platinum particles with carbon nanotube layers

Platinum(Pt) is a typical catalytic metal and size-reduction of the particles enhances the catalytic activity. Recently the importance is very much increased for the application to a catalyst on electrodes of a fuel cell. The microstructure and the interfaces with various kinds of supports have to be elucidated in an atomic resolution. The present study was focused on the reaction of Pt particles with a layer of carbon nanotubes(CNT). The CNT layer sample was prepared by the method developed by one of the present author[10], where hexagonal silicon carbide(SiC) particles were heated at 1700 C by heating in a vacuum furnace for forming CNT layer around each SiC particle. Platinum was then deposited on the layer by using DC sputtering outside of the RSHVEM. The composite particles were dispersed onto a tungsten spiral wire used as an electrical resistance heater. The sample was inserted into the microscope and observed in-situ at 1000 C with oxygen gas of 1.8×10^{-4} Pa.

During the in-situ HVEM observation, the Pt particles reacted with the surface of CNT layers, the surface was etched gradually by desorption of carbon atoms and finally the Pt particles sank into a lower side of the layer as shown in Fig. 8[11]. We also succeeded in the in-situ observation of oxidation process of the surface of CNT layers in atomic level.

(A-3)Fracture process of Cu/Si interfaces

LSI and MEMS devices contain various kinds of nm-sized components and their interfaces. The mechanical strength of such interfaces, owing to the extreme smallness of the components, is believed to be sensitive to the foreign gas atoms which are diffusively supplied from an outer environment. Particularly, the effect of hydrogen on interfacial strength will become an important issue as it is known as a typical embrittling species. By using the RSHVEM, we have tried in-situ observation of fracture process of a semiconductor/metal interface in various kinds of gas atmospheres including hydrogen.

The present TEM sample including a micro cantilever was prepared from sputter-deposited multilayers using a standard focused ion beam(FIB) instrument as shown in Fig. 9(a). The cantilever sample is composed of carbon(C), silicon nitride(SiN), copper(Cu) and silicon(Si) layers. The sample was mounted on a gold wire and attached to a piezo-driven nanoindenter specimen holder (Nanofactory Inc.). The hardest SiN layer was pressed by a diamond indenter tip in order to avoid plastic deformation at the loading point. During the load application, fracture initiation from the Cu/Si interface edge was particularly focused. The atmospheric gas and pressure were N_2/H_2 mix gas(95:5) and 300 Pa, respectively. In situ-observation revealed that the fracture initiated at the upper edge of the Cu/Si interface as shown in Fig. 9(b), and it propagated to the bottom edge of the interface within the frame rate of 1/30 s. Simultaneously, we successfully measured the applied load as shown in Fig. 10; the fracture load of the Cu/Si interfaces in the atmosphere was measured as P_c =75.3 μN. Such a quantitative data then allows us to calculate the local fracture stress at the Cu/Si interface edge by using a numerical analysis, e.g. finite element method, which is necessary for strength evaluation.

(B) Elemental and chemical mapping using post column EELS and energy filter

(B-1)Energy-filtered TEM of oxide multilayers

Elemental distribution images can be obtained by using a post-column type energy filter of the present RSHVEM. Figures 11(a) and (b) show energy-filtered cross sectional TEM (EF-XTEM)

images of a multilayer of $PrMnO_3$, $SrTiO_2$ and $LaMnO_3$ using the Ti-$M_{2,3}$ core-loss spectrum respectively taken by a high-resolution TEM at 200kV and the present RSHVEM at 1 MV. The energy slit width used was 5 eV and the recording time was 2 seconds for both images, with the edge jump ratio (two-window) method applied. The present example illustrates accelerating voltage dependence of the image delocalization effect of inelastically scattered electrons. The Egerton's formula [13] predicts similar spatial resolution of 0.4-0.5 nm for the filtered images both at 1 MV and 200 kV using an energy loss of ~50 eV, because the advantage of smaller wavelength for the higher energy is compensated for by the smaller characteristic angle of inelastic scattering. The EF-TEM image at 1 MV, however, exhibits sharp interfaces between the $SrTiO_3$ layer and $PrMnO_3$ and $LaMnO_3$ layers containing no Ti, whereas the $SrTiO_3$ layer shows a significant blunt feature for 200 kV in Fig. 11(a), as expected by the Egerton's formula. This clear difference could be attributed to less beam broadening in the sample for higher voltages. It should be noted that the lattice-like fringes in $SrTiO_3$ of Figure 11(b) do not mean atomic column resolution of the method but results from interference effects of inelastic scattering, as judged from the corresponding ADF-STEM image in Fig. 11(c). The present example demonstrates another advantage of using HVEM: EF-TEM image with better spatial resolution can be obtained with less recording time using core loss edges of lower energy region, compared with those obtained by medium voltage instruments. Higher voltages increase the mean free path for the inelastically scattered electrons, which even facilitates the low loss region to utilize for EF imaging. In Fig. 11(b), the filtered image using Ti-M_{23} edge gives 0.5 nm, which is best resolution ever obtained using the core loss edge at less than 50 eV, which could be substantially better than the record obtained by a 300 kV instrument equipped with an in-column type energy filter, using the oxygen K-edge (< 500 eV) [14].

(B-2) Chemical state mapping of semiconductor device by STEM-EELS

To demonstrate another capability of HVEM-EELS spectrum imaging (SI) by using STEM was attempted for a thick semiconductor sample, because high through-put analysis of devices for real-use is demanded and the typical sample thickness prepared by FIB can be ~100 nm, which could be thicker by a factor of two than that usually appropriate for EELS. As described already, the mean free-path for inelastic scattering is larger by a factor of 1.5 than that of medium voltage instruments, which allows us to examine thicker samples.

The cross-sectional sample of a gate area in CMOS-FET of 100 nm sample thickness was scanned by a probe of ~2 nm with a step interval of 5 nm and a 'datacube' of 128 x 93 pixels^2 x 2048 channels with the energy dispersion of 0.1 eV/channel including the ZLP. The parent datacube was processed by first aligning the spectra using the ZLP, Fourier-log deconvolved to remove the plural scattering, followed by isolating the Si-$L_{2,3}$ edge subtracting the pre-edge background using the power-low modeling. The ROI includes different silicon compounds and the multivariate curve resolution (MCR)

technique was applied to the dataset for separating the mixed spectra into the pure components and their spatial distributions at the same time [15]. Figures 12(a)-(e) show the resolved spectral components, their spatial distributions and the residual (noise) resulting from the 3-component MCR processing. It is apparent from the resolved spectral profiles that Figs. 12(b)-(d) respectively correspond to crystalline Si, SiO_2 and Si_3N_4. Note that this chemical mapping was done with no reference spectra. It should be also mentioned that such analysis is not feasible by 200 kV instruments because the Si-$L_{2,3}$ edge is smeared out by the tail of plasmon peaks at this thickness.

(C) Three-dimensional reconstruction

(C-1)Carbon micro coils in TEM

A carbon micro coil(CMC) is a potential material for absorbance of electromagnetic waves for various kinds of shielding, and it is different from a carbon nanotube discovered by Iijima[16]. A holographic observation of the electrostatic field caused by currents along the coil was made by Yamamoto et al.[17], but the growth process is still not clarified, because the details of the 3D structure are unknown. The present sample was prepared by a CVD method using acetylene gas and catalyst of nickel-alloy particles[18]. The CMC was mounted onto a thin metal wire by using deposition of tungsten as a glue in a FIB instrument. The sample holder of the RSHVEM was a newly developed one for 360 degree full rotation. The tomographic images were recorded by 1 degree step from 1 to 180 degree in one rotation axis.

Figure 13 shows a tomographic image reconstructed from 180 bright field images, which shows clearly a 3D structure and the cross-section of the coil. This is because the linearity between the image contrast and projected potential (thickness) holds in thicker areas at 1 MV HVEM than that by ordinary 200 kV TEM[19]. Series of the observation may clarify also the growth process of the coil.

(C-2)Chromosome in TEM

In ordinary electron microscopy of biological cells at 100 kV accelerating voltage, where the maximum thickness is about 0.1 micrometer, the whole cell of about 5-10 micrometer in thickness is difficult to observe clearly, and therefore it has to be sliced by using a microtome. In HVEM the large transmittance of electron enables observation of biological samples over 5 micrometer thickness. The whole cell observation is very valuable of biological science. The chromosome sample in mitotic phase was prepared by a specially developed method for observation of whole cell, where soluble proteins and cell membranes were removed, remaining cytoskeletal filaments and chromosome were fixed with 1 % glutaraldehyde and $MoOsO_4$ and then freeze-dried. Figure 14 shows a

pick-up from a series of tomographic images of the chromosome in the NRK cell of a rat in M-phase, where the spindles appear in order to separate a pair of the chromsome. The tomographic reconstruction reveals the whole 3D structure of the chromosome and connection of the surrounding spindles, which was discovered to be composed actin filaments[20].

(C-3)Yeast cell in ADF-STEM

High-voltage electron microscope (HVEM) is valuable for thicker samples as already shown. However, inelastic scatterings of electrons make an image blurry. Especially, it is too difficult to get high-contrast images in thicker biological samples. The RSHVEM has energy filtering and scanning image functions. Energy filter can make a sharp image by filtering out inelastic electron scattering coming from thicker specimens. On the other hand, STEM images give integrated amplitude contrast along specimen depth in each spot scanned on the specimen. We use a budding yeast (Saccharomyces cereviciae) cell which diameter is approximately 3 μm as a biological sample to observe a whole cell structure. The sample was embedded in epoxy resin after chemically fixed and sectioned at ~3 μm thickness. The image of the thicker biological specimen was observed by using energy filtering and the STEM function at an accelerating voltage of 1MV. Figure 15 is the bright field STEM image, which showed higher-contrast and sharper images than that of energy filtering TEM images. Tomography using STEM images gave three-dimensional structures of a whole yeast cell in which the shape and the distribution of major organelles of nucleus, vacuoles, and mitochondria are identified inside the cell. High-voltage STEM tomography showed a potential to visualize a whole cell structure in one observation. The technical details will be discussed in other paper[21].

<Ref. J.C. Bouwer et al., J. Struct. Biol., 148 (2004), 297>　最後に削除します。

4. Comparison with another environmental TEM method using module tips

As already noted, there are two methods for environmental observation in TEM and STEM, such as those using the closed type cell and the open type cell. Since 1990's[5], high resolution environmental TEM(ETEM) studies have been performed by using the open type cell. Because the membrane may be a strong obstacle for clear-cut observation, and inelastic scattering in the film degrades the image resolution and contrast. In the present RSHVEM, we used the open-type cell, and the resolution less than 0.2 nm was successfully obtained in gaseous conditions, as expected. However, the cost of the system is very high. Recently, various kinds of modules for closed type environmental cells were developed for high resolution ETEM and E-STEM. Particularly interested is dark field

STEM observation of gold particles in gas or liquid, where the (111) lattice planes of 0.235 nm was resolved[22]. This is because STEM can evade deterioration of images caused by inelastic scattering in membrane films and atmospheres, because no imaging lenses exist. However, use of the modules particularly for observation in liquid such as water may be very risky for maintenance of instruments. Once the membranes are broken, accelerating anodes and electron guns should be fatally damaged. For the safety, even in use of the closed type module, instruments equipped with a differential pumping system are recommended to be used. The easy use of the closed type modules for environmental observation is realized by the recent development of MEMS technology, which gives us further various kinds of manipulation of samples and in-situ measurements of physical properties.

5. Propose of "*in-place* observation" for reducing irradiation effects onto specimens

One of the most important problems to be considered is the effect of irradiation of ions of atmospheric gasses produced by electron irradiation inside the cell. The effect is increased with that of gas pressure. Ordinary chemical reaction is sufficiently occurred in lower atmospheric pressures such as a few Pa, and so we may be able to study various kinds of the reaction without so much heavy ion irradiation. In case of adsorption of molecules, however, the situation is serious. There is a definite limitation of decrease of electron intensity onto samples in viewpoint of quantum noise of imaging. As one of solution of the problem, we would like to claim the importance of "in place" observation, where electron beam is timely off during the chemical reaction between samples and gases. For the high-resolution in-place observation, a reliable beam blanking system is equipped in the present RSHVEM[2]. The blanking is performed with electrostatic deflectors above the third condenser lens. The command of the blanking is computer-controlled and programmed with the link of gas-injection and evacuation for in-situ chemical reaction. We have succeeded in perform "in place observation" of (200) lattice images of a gold film in the present instrument at 1 MV without a large amount of sample drift. The technology should be used for ordinary environmental TEM at 200-300 kV accelerating voltages.

6. Conclusion

In the present paper, development of a new HVEM for reaction science is described in detail and some application data are presented in order to show advantages of HVEM for in-situ and environmental observation of thicker samples. Also TEM images using core loss electrons with the imaging filter reveals the superiority of image localization of

interfaces of oxides. An effective signal processing method for STEM-EELS mapping is shown for elemental analysis of a semiconductor. All of the data were obtained by the new RSHVEM in Nagoya University at 1 MV accelerating voltage. The instrument have contributed many other studies on metallugical[23], catalytic[24] and chemical reactions These data refurbish previous HVEMs, whose characteristic is mainly observability of thicker samples. Finally, we have claimed the importance of " in place observation", where electron beam is smartly blanked during a chemical reaction, as well as ordinary " in-situ observation" for the studies of various kinds of advanced materials.

Acknowledgements

The authors would like to make sincere thanks to Dr. S. Hirano, the past president of Nagoya University(NU) and Dr. T. Matsui, the past director of the Ecotopia Science Institute(ESI) for their efforts to acquire the grant for development of the RSHVEM, as well as to Prof. H. Mori of Osaka University for his dedicated support to this project. We also acknowledge Prof. M. Hamaguchi, the current president of NU for his heartily support to the HVEM facility. The instrument was completely installed with the best performance by JEOL Ltd., and particularly Dr. S. Ohta and Mr. M. Ohsaki are acknowledged for their efforts. We greatly thank to Dr. Y. Takahashi at Kasai University, Dr. J. Yamasaki of NU, Dr. I. Ohkubo (Presently, National Institute of Materials Science), Dr. Y. Sakurai and Dr. N. Harada of University of Tokyo, and Dr. K. Murata at National Institute for Physiological Sciences(NIPS) for providing their data of fracture, carbon micro coils, semiconductor oxides and yeast cells, respectively, to this paper. The development of the RSHVEM was fully supported by the Ministry of education, science, culture and sport (MEXT) in Japan .

References

1. Dornfeld D (2012), "Green manufacturing - Fundamentals and application -" (Springer, Berlin).

2. Tanaka N, Usukura J, Kusunoki M, Saito Y, Tanji T, Muto S, Arai S (2010), Development of high voltage electron microscopy for reaction science, Int. Microscopy Congress-17(Rio de Janeiro), I9-2.

3. Fukami A and Katoh A (1972), Construction and application of environmental cell, Proc. 30th EMSA meeting (Los Angeles), ed. Arceneaux ?? (Baton Rouge Publishing).

4. Gai P L and Boyes E (200X), "Electron microscopy for heterogeneous catalysis", (IOP Press, Bristol).

5. Sharma R (2001), Design and applications of environmental cell transmission electron

microscope for in-situ observations of gas-solid reactions, Microscopy and microanalysis, 7, 494-506.
6. Hansen P L, Wagner J B, Helveg S, Rostup-Nielsen J R, Clausen B S and Topsoe H (2002), Atom-resolved imaging of dynamic shape changes in supported copper nanocrystals, Science, 295, 2053-2055.
7. Yoshida H. Uchiyama T and Takeda S (2007), Environmental transmission electron microscopy of swinging and rotational growth of carbon nanotubes, Jpn J. Appl. Phys., 46, L917-L919.
8. Bright A N, Yoshida K and N. Tanaka N (2012), Influence of total beam current on HRTEM image resolution in differentially pumped ETEM with nitrogen gas, Ultramicroscopy, http://dx.doi.org/10.1016/j.ultramic.2012.08.007
9. Kamino T, Yaguchi T, Konno M , Watabe A, Marukawa T, Mima, T, Kuroda K, Saka H, Arai S, Makino H, Suzuki Y and Kishida K, Development of gas injection/heating holder for use with transmission electron microscope, J. Electron Microsc., 54, 497-503.
10. Kusunoki M, Suzuki T and Hirayama T and Shibata N (2000), A formation mechanism of carbon nantube films on SiC(0001), Appl. Phys. lett., 77, 531-533.
11 Matsuda K, Norimatsu W, Kusunoki M and Arai S (2012), Patterning of aligned CNT films using SiO_2 particles monolayer as a mask, e-J Surf. Sci. Nanotech., 10, 198-202.
12. Takahashi Y, Arai S, Yamamoto Y, Kondo H, Tanaka N, Effect of gas environment on interfacial fracture strength of micro components (2012), submitted to Scr. Mater.
13 Egerton R F "Electron energy loss spectroscopy in the transmission electron microscope" (Prenum Press, New York)
14. Bando Y, Mitome M, Golberg D, Kitami Y, Kurashima K, Kaneyama T, Okura Y and Naruse M (2001), New 300 kV energy-filtering field emission electron microscope, Jpn. J. Appl. Phys., 40, L1193-L1196.
15. Muto S, Yoshida T and Tatsumi K (2009), Diagnostic nano-analysis of materials properties by multivariate curve resolution applied to spectrum images by S/TEM-EELS, Mater. Trans, 50, 964-969.
16. Iijima S (1991), Helical microtubules of graphitic carbon, Nature, 354, 56-58.
17. Yamamoto K, Hirayama T and Kusunoki M (2006), Electron holographic observation of micro-magnetic fields current-generated from single carbon coil, Ultramicroscopy, 106, 314-319.
18. Motojima S, Kawaguchi M, Nozaki K and Iwanaga H (1990), Growth of regularly coiled carbon filaments by Ni catalyzed pyrolysis of acetylene and their morphology

and extension characteristic, Appl. Phys. Lett., 56, 321-323.
19. Yamasaki J(2012)
20. Usukura J(2011)
21. Murata K.(2012)
22. Allard L(2009), Application of high resolution aberration corrected STEM imaging to studies of the behavior of nanophase materials at at elevated temperatures, Proc. Microscopy and Microanalysis, 15, 130.
23. Sasaki, K,
24. Fujita T, Guan P, McKenna K, Lang X, Hirata A, Zhang L, Tokunaga T, Arai S, Yamamoto Y, Tanaka N, Ishikawa Y, Asao N, Yamamoto Y, Erlebacher J and Chen M, (2012), Atomic origins of high catalytic activity of nanoporous gold, Nature mater. DOI: 1-:1038/NMAT3391.

Figure captions

Fig. 1: Illustration of a general view of reaction science high voltage electron microscope(RSHVEM).

Fig. 2: Vacuum characteristics of gas-introduction and re-evacuation processes.

Fig. 3: High-resolution of a [110] oriented cubic silicon carbide crystal, whose dumbbell structure of 0.109 nm is resolved.

Fig. 4 Energy filtered image of Ce_2O_3 particle using M_{23} edge of cerium.

Fig. 5: (200) lattice fringes of a gold film in vacuum(a) and in nitrogen gas of 11,000 Pa(b) at 1 MV.

Fig. 6: Low magnification image of copper (Cu) particles deposited on silica particles before oxidation and reduction processes.

Fig. 7: Series of EELS in oxidation and reduction processes.

Fig. 8: Reaction of platinum particles and a carbon nanotube layer in oxygen atmosphere of 1.8×10^{-4} Pa at 1000 ℃.

Fig. 9: In-situ fracture process initiated by a piezo-driven tip (upper right) in hydrogen atmosphere. Low magnification image of a cross section sample of a vacuum-deposited C/SiN/Cu/Si multilayers. (a) Before loading and (b) after loading in hydrogen atmosphere.

Fig. 10: Diagram of load against time, which determined that the maximum stress of fracture is 75 μN.

Fig. 11 Energy filtered TEM image of multilayered oxide, which insights the image delocalization effects. (a) Image at 200 kV, (b) that at 1 MV obtained of the RSHVEM,

and (c) ADF-STEM image at 200 kV.

Fig. 12: STEM -EELS images showing different chemical states of a semiconductor.

Fig. 13: three-dimensional TEM image of a carbon micro coil (CMC)

Fig. 14: A pick-up of three-dimensional tomographic image of a chromosome of a rat obtained in TEM mode of the RSHVEM.

Fig. 15: A pick-up of three-dimensional tomographic image of a yeast cell obtained in bright field STEM mode at 1 MV.

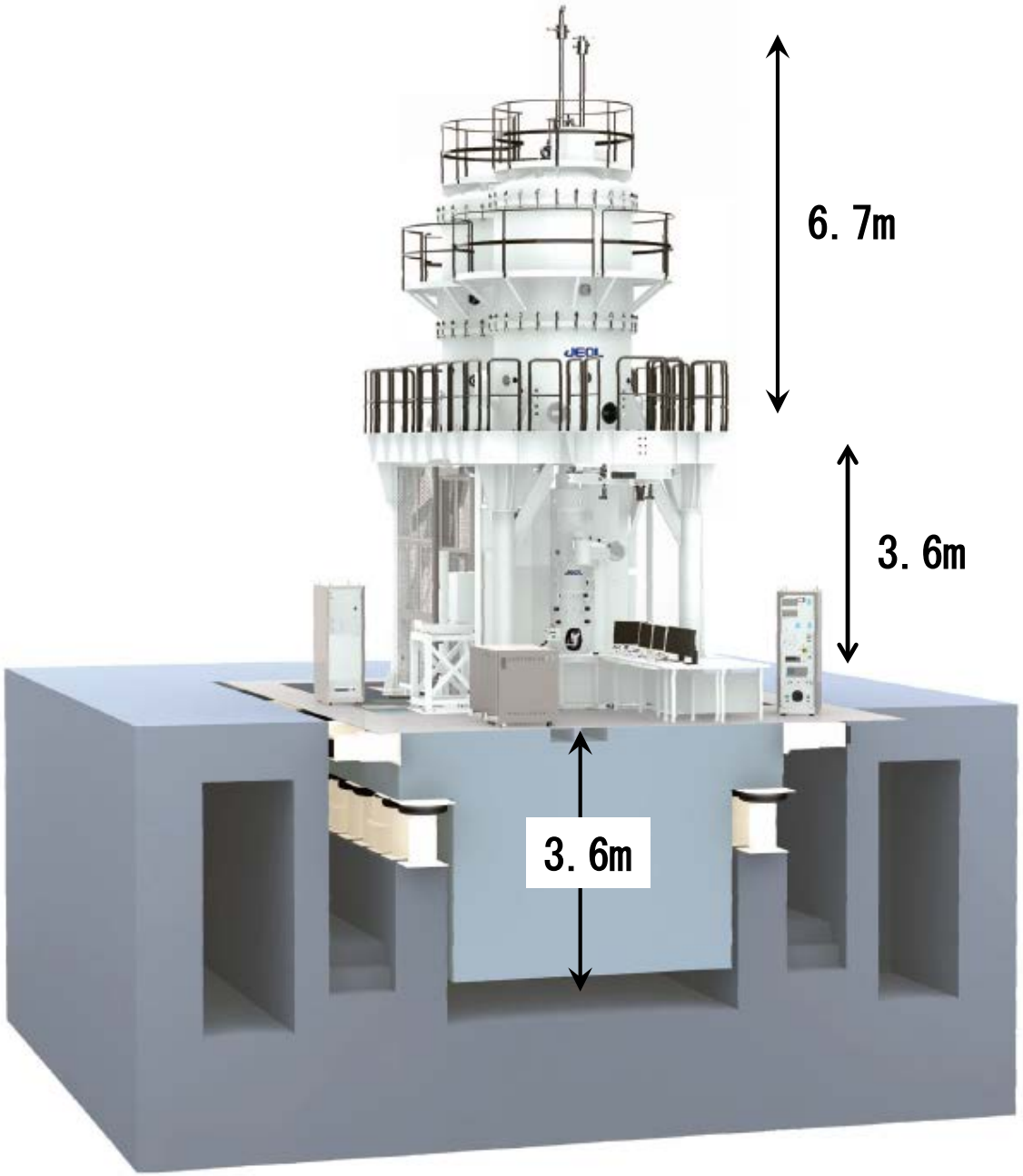

Fig. 1 Tanaka et al

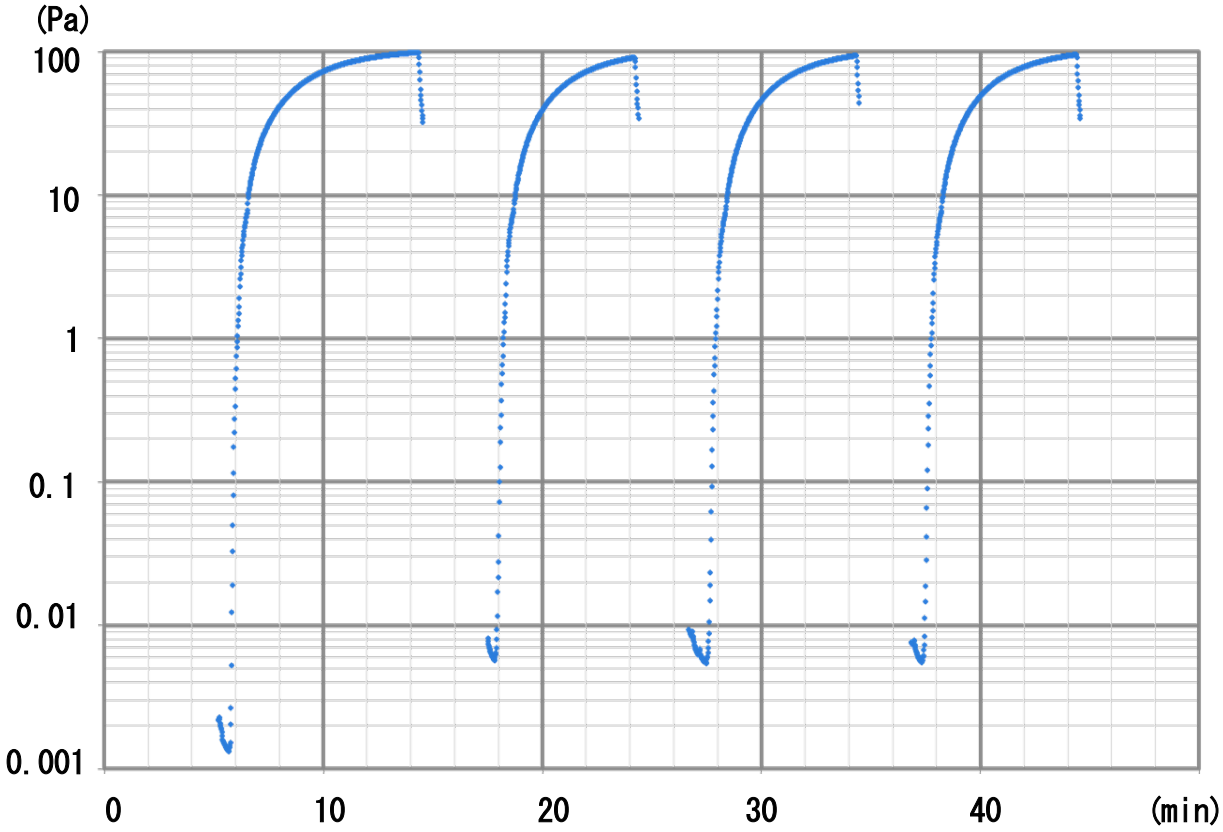

Fig. 2 Tanaka et al

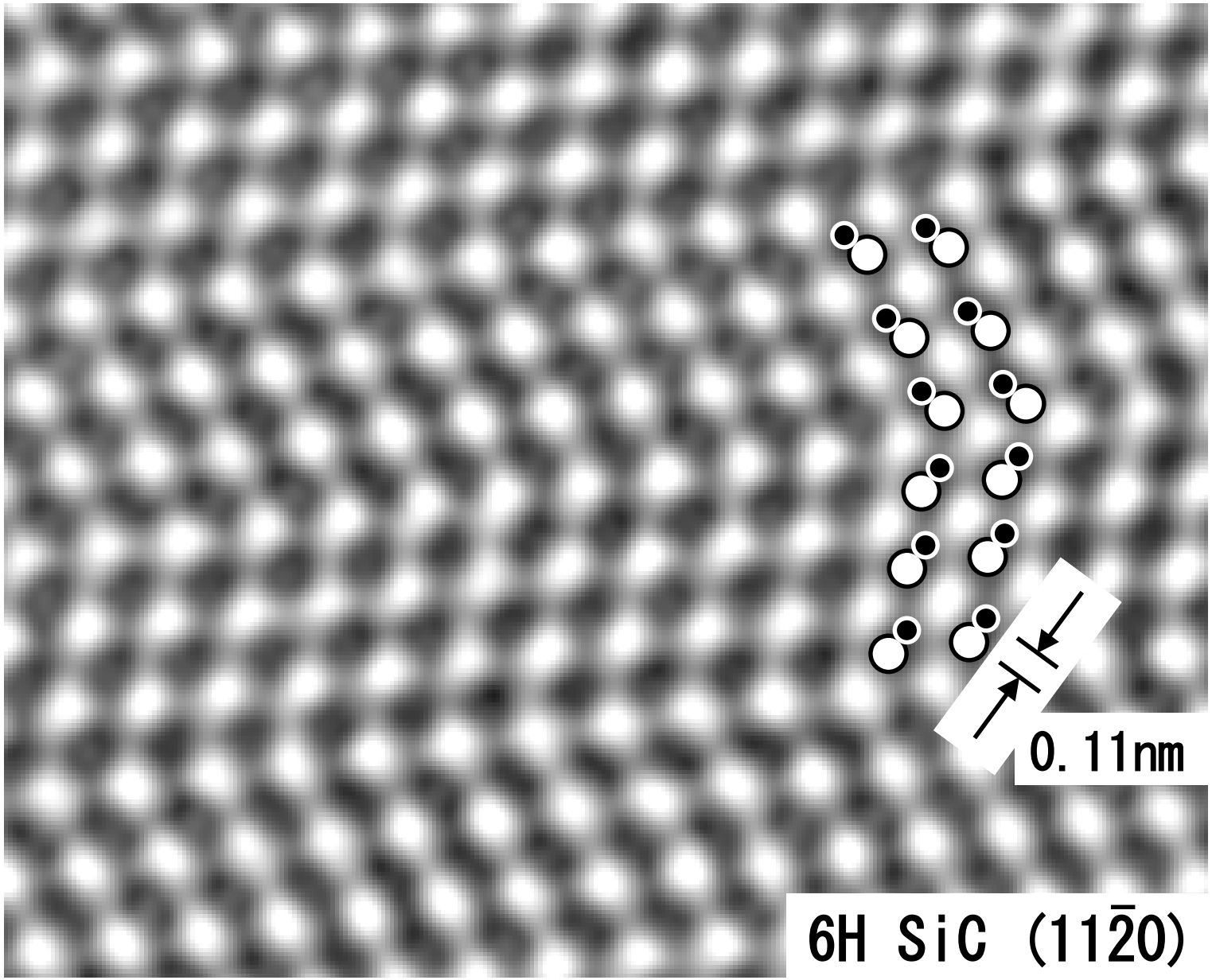

Fig. 3 Tanaka et al

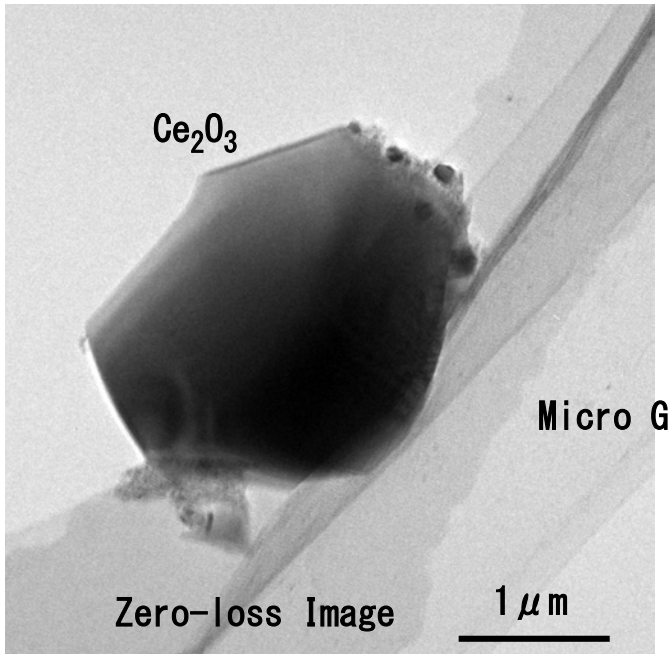

Fig. 3 Tanaka et al

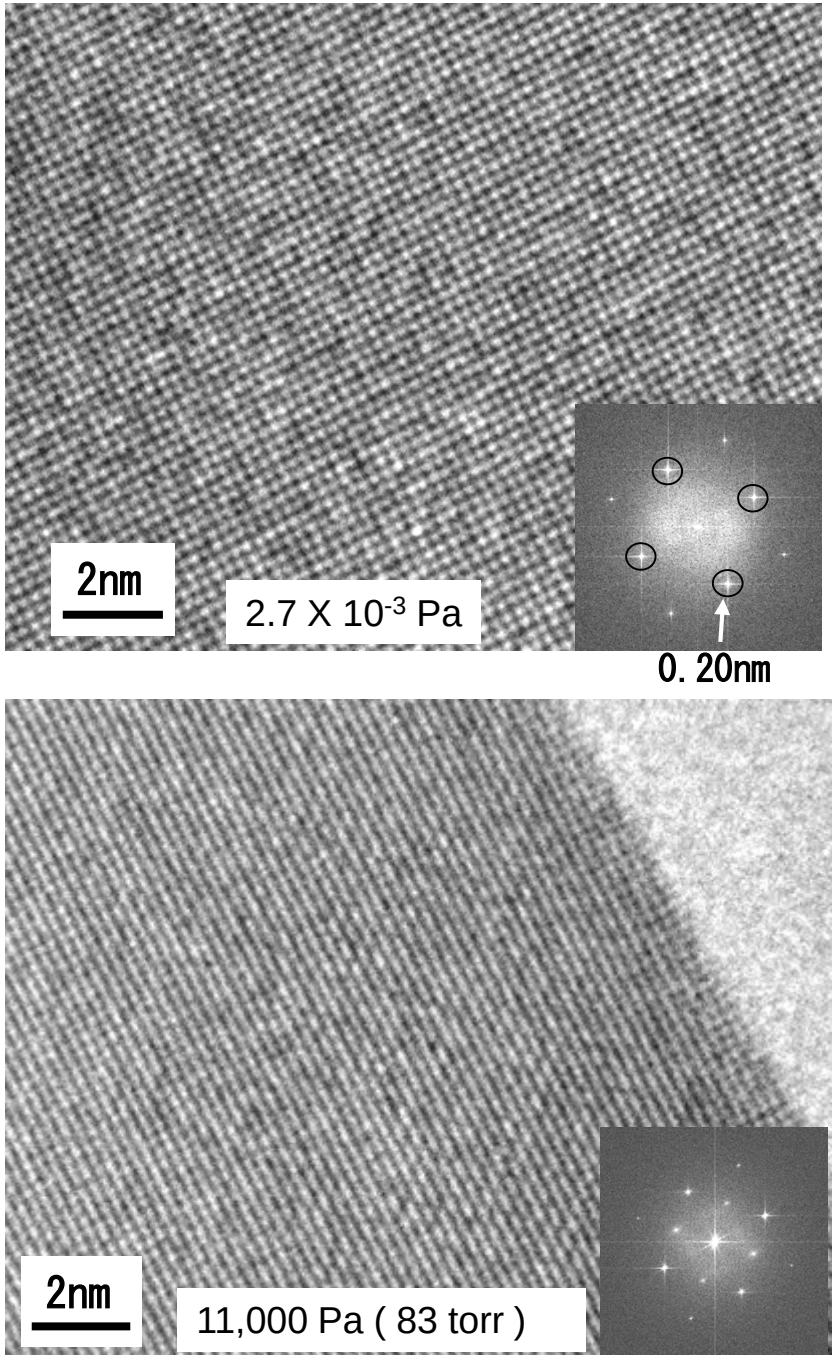

Fig. 5
Tanaka et al

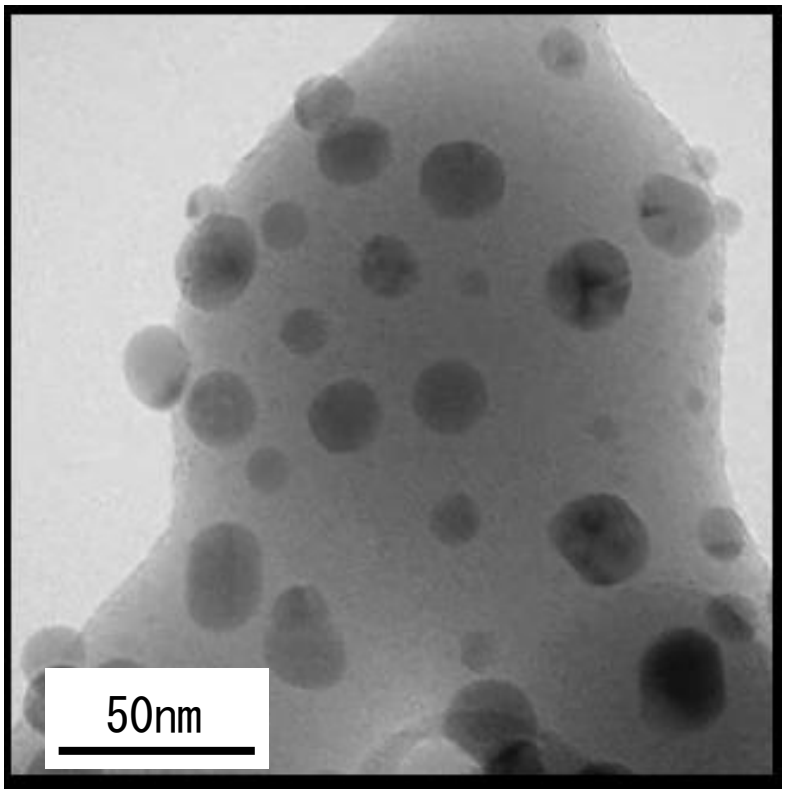

Fig. 6 Tanaka et al

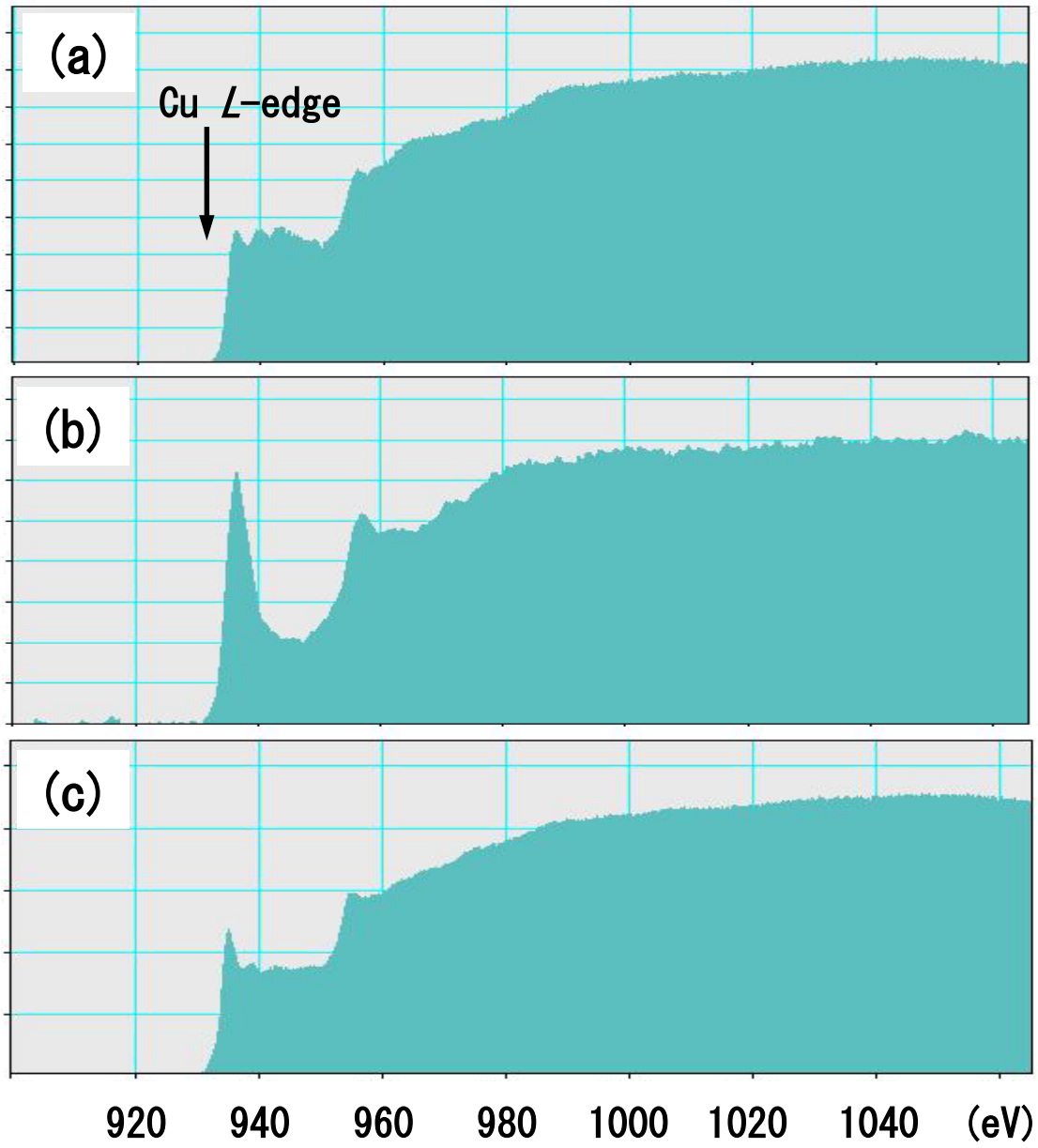

Fig. 7 Tanaka et al

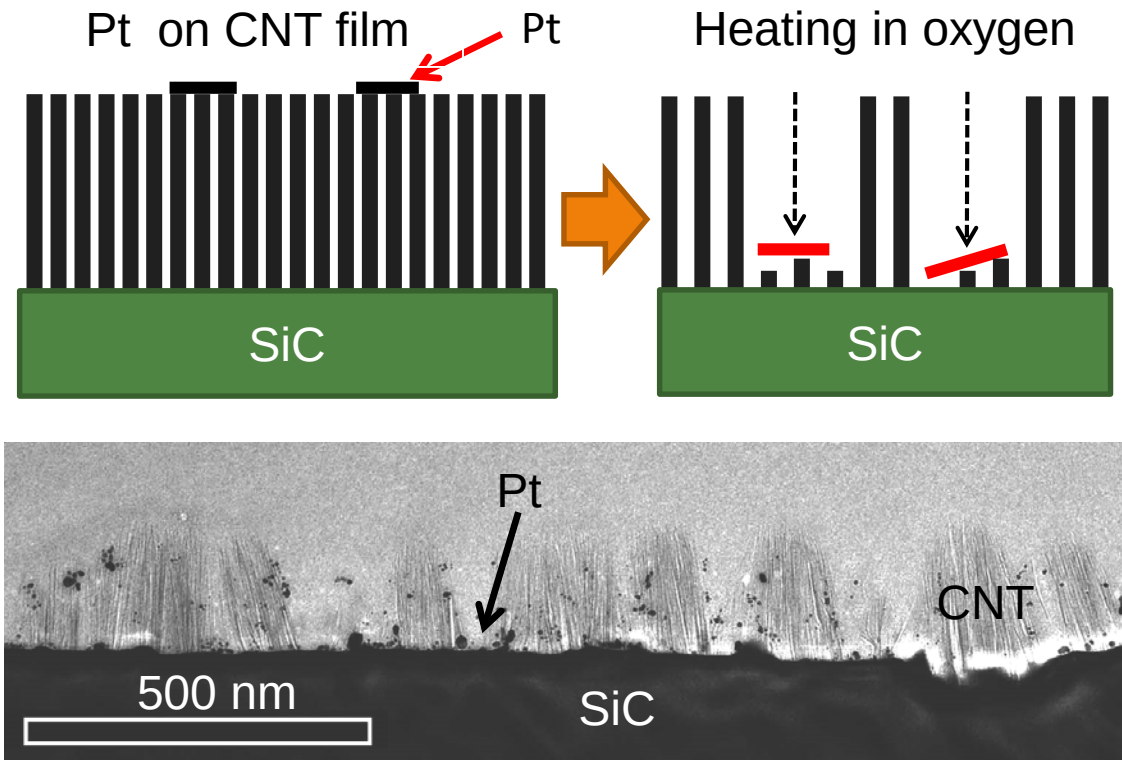

Fig. 8 Tanaka et al

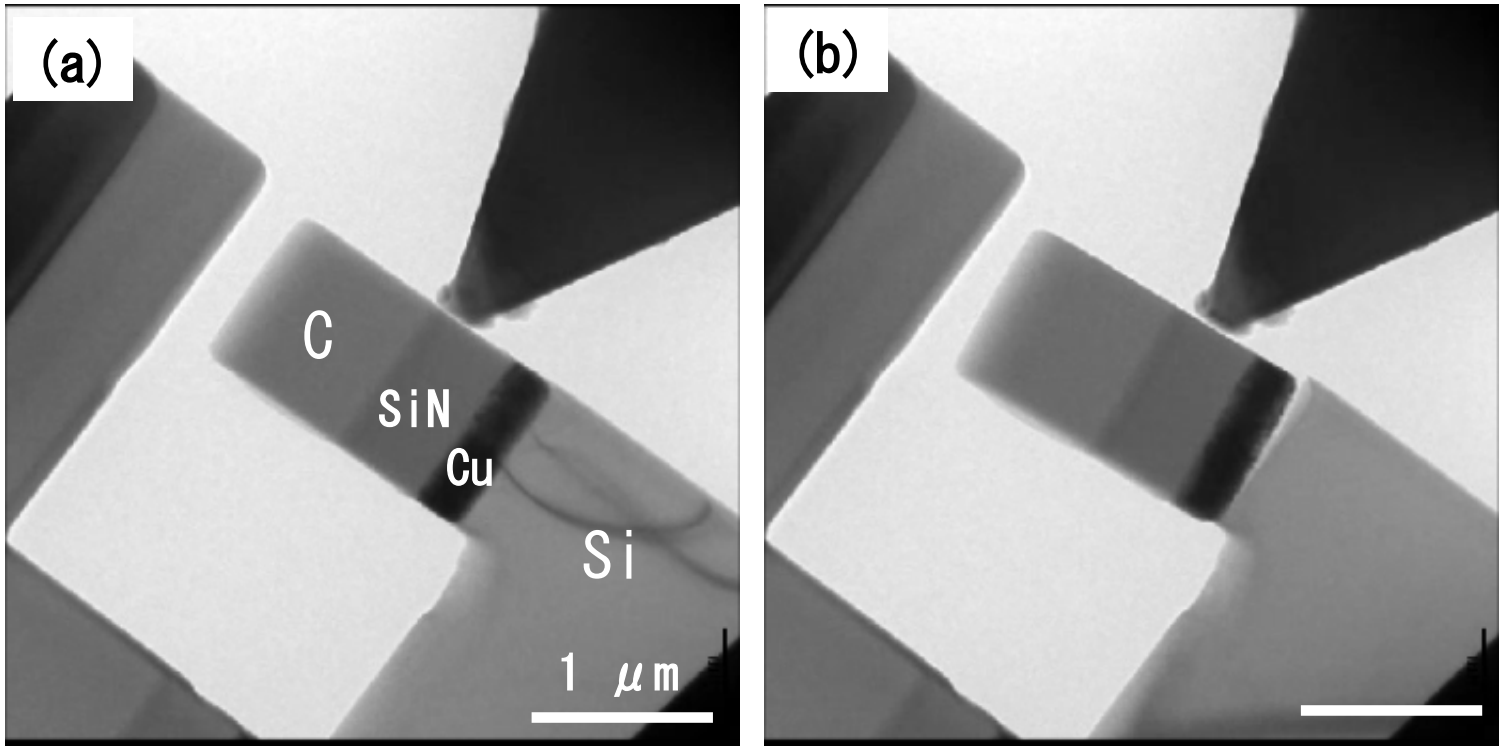

Fig. 9 Tanaka et al

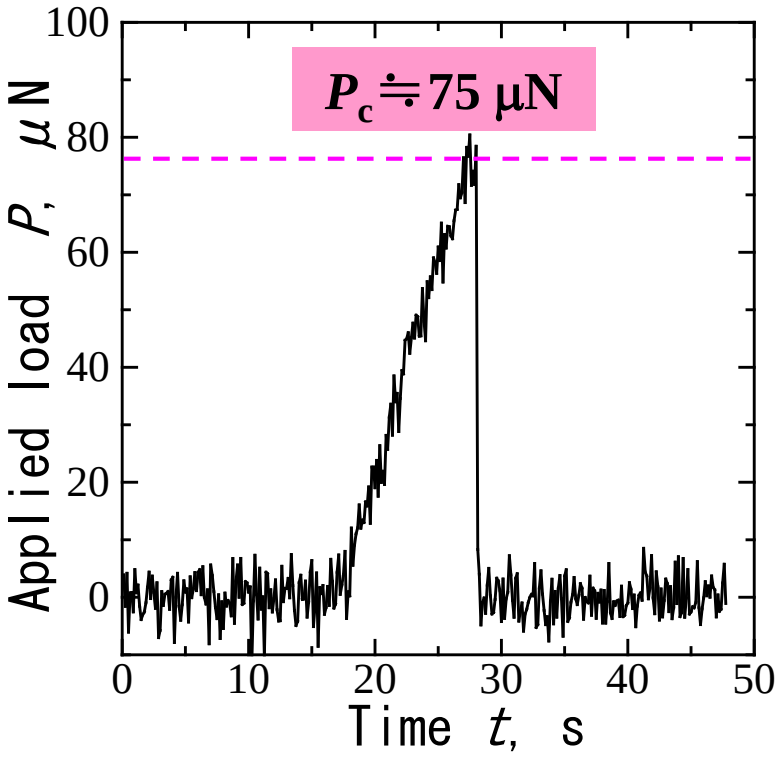

Fig. 10 Tanaka et al

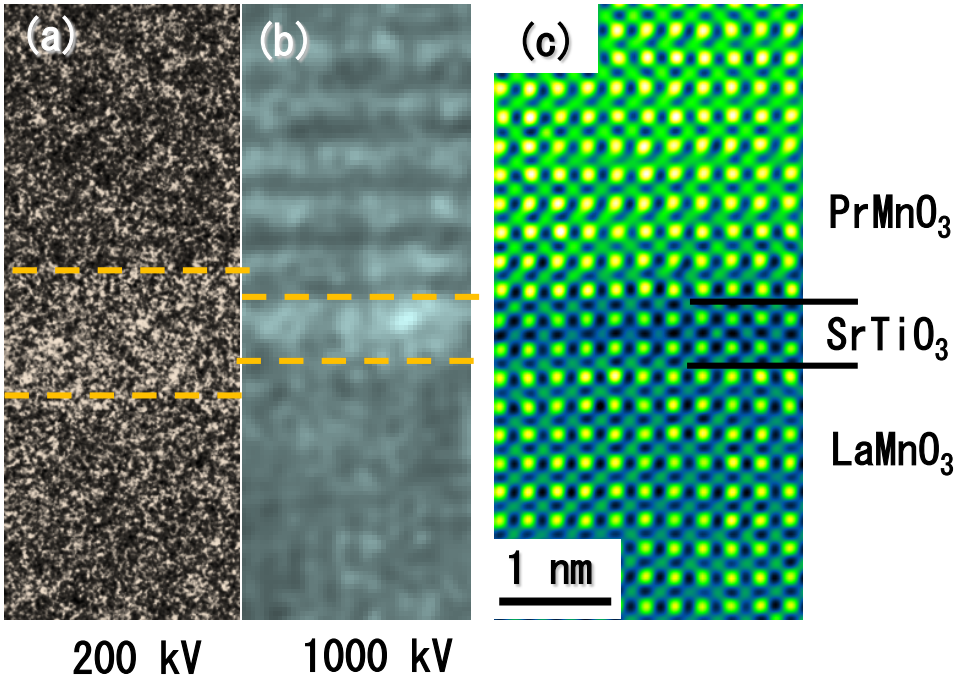

Fig. 11 Tanaka et al

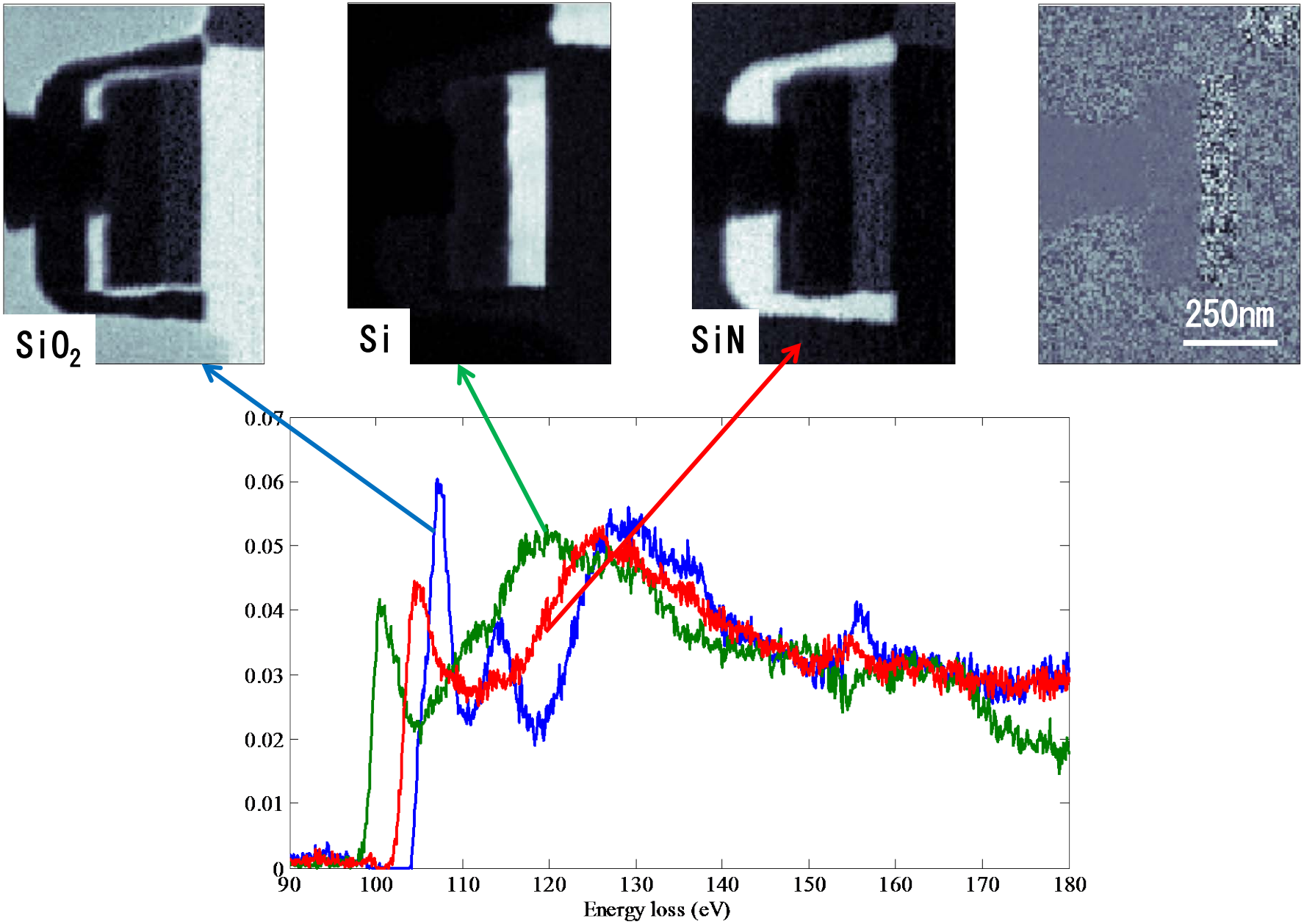

Fig. 12 Tanaka et al

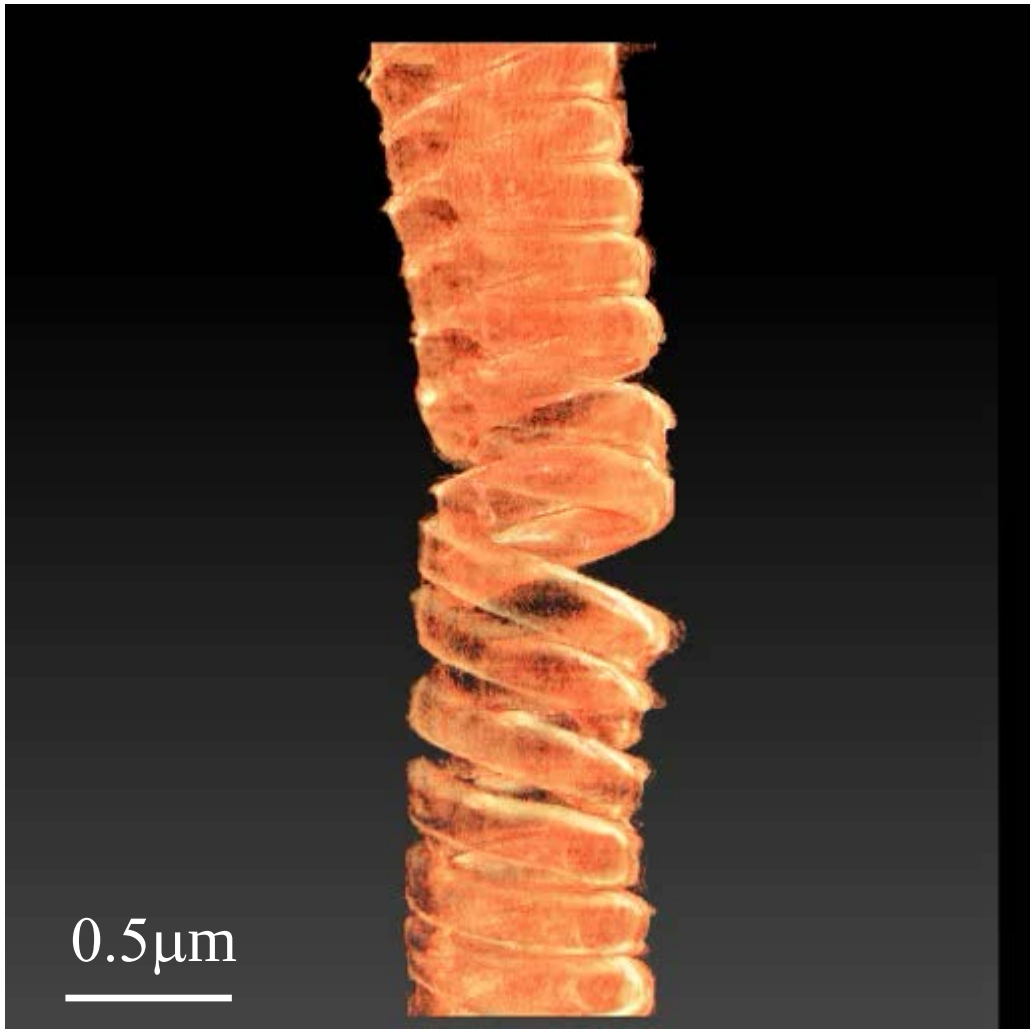

Fig. 13 Tanaka et al

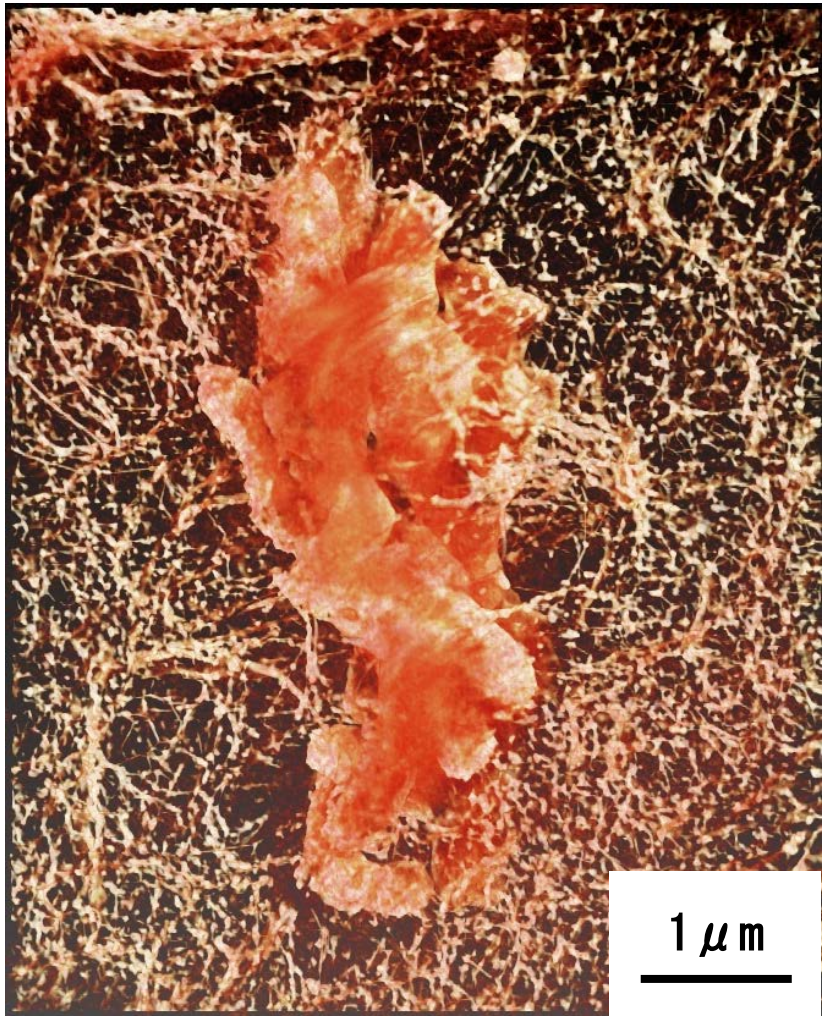

Fig. 14 Tanaka et al

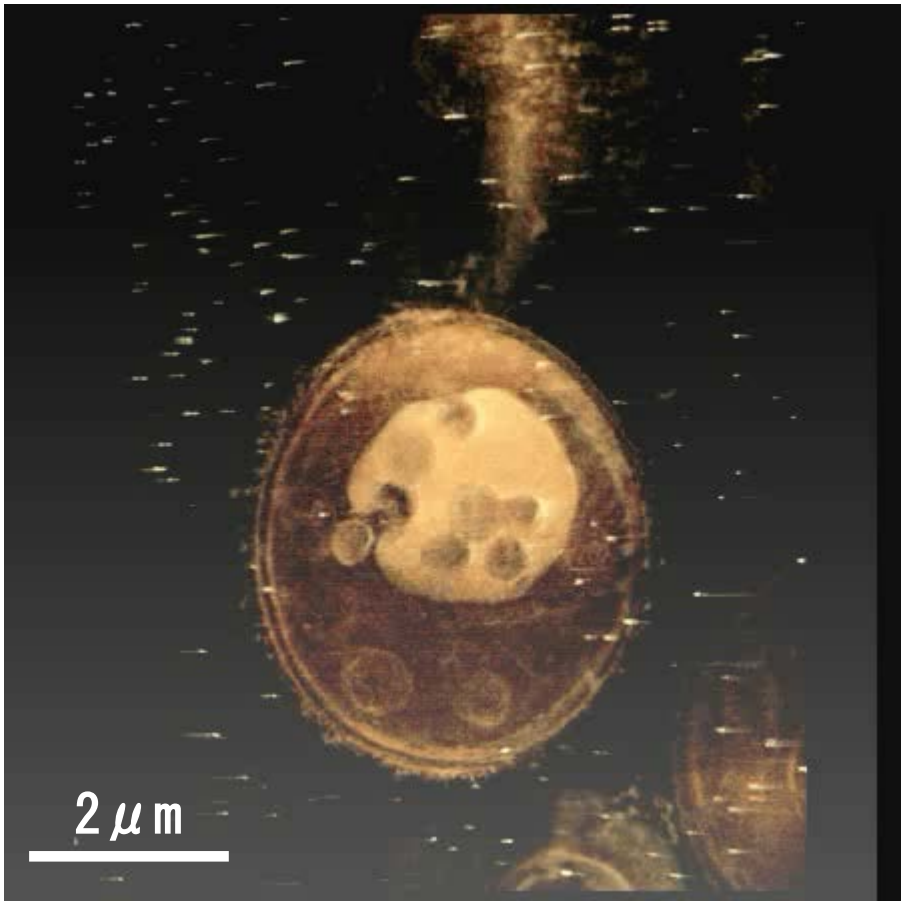

Fig. 15 Tanaka et al

Fig. 7 Tanaka et al

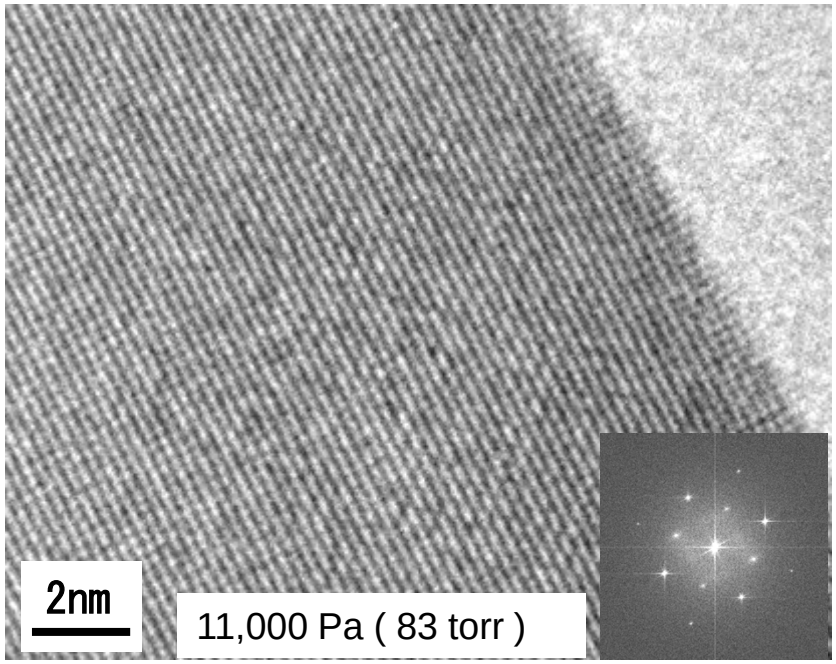

Fig. 4 Tanaka et al